Cell Reports, Volume *24*

Supplemental Information

Epithelial-Mesenchymal Transition Induces Podocalyxin to Promote Extravasation via Ezrin Signaling

Julia Fröse, Michelle B. Chen, Katie E. Hebron, Ferenc Reinhardt, Cynthia Hajal, Andries Zijlstra, Roger D. Kamm, and Robert A. Weinberg

Figures S1-S6

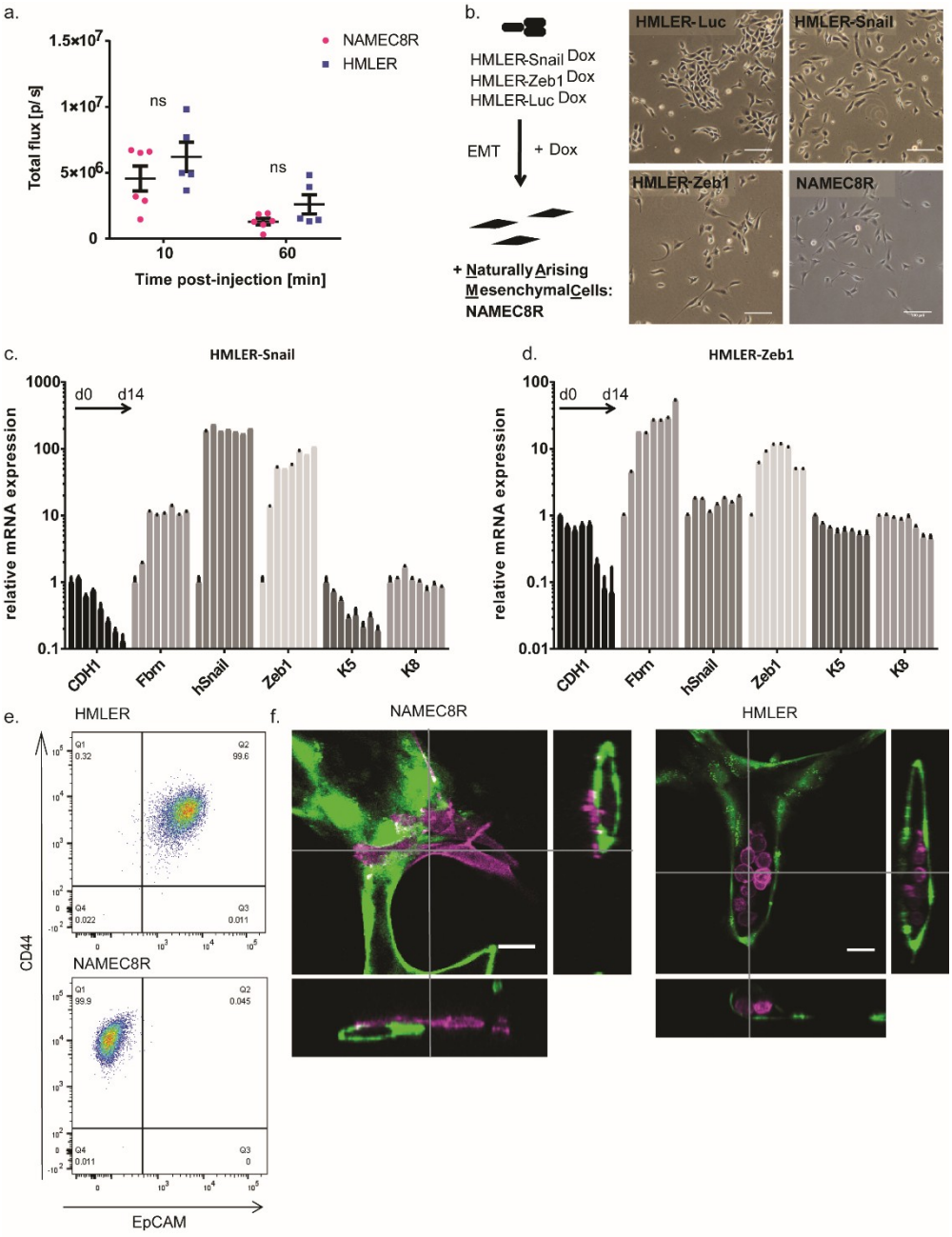

Figure S1: Extended characterization of breast cancer cell lines. Related to Figure 1. (a) Bioluminescent imaging of mice 10 or 60 min after injection with NAMEC8R or HMLER cells expressing a luciferase-tdTomato fusion gene shows no significant differences in cell numbers in lungs of mice. n=5-6. Data are represented as mean ± SEM. (b) EMT induction in HMLER cells *in vitro*. Left: HMLER cells were forced to undergo an EMT by dox-inducible overexpression of either Snail or Zeb1 EMT-TF. Dox-inducible expression of *Renilla* luciferase served as a negative control and NAMEC8R cells as a positive control. Right: representative bright-field images of HMLER-Luc, -Snail, -Zeb1 cells treated with dox for 14 d in comparison to mesenchymal NAMEC8R cells. Scalebars: 100 µm. (c,d) mRNA expression of EMT markers in HMLER-Snail (c) and HMLER-Zeb1 (d) cells throughout a 14 d treatment with dox *in vitro* (2d time intervals). (e) Flow cytometric analysis comparing CD44 and EpCAM levels on HMLER and NAMEC8R cells. (f) Orthogonal views of NAMEC8R and HMLER cells (purple) extravasated from or stuck in microvascular networks (green) *in vitro* (t=4h). Scalebars: 30 µm.

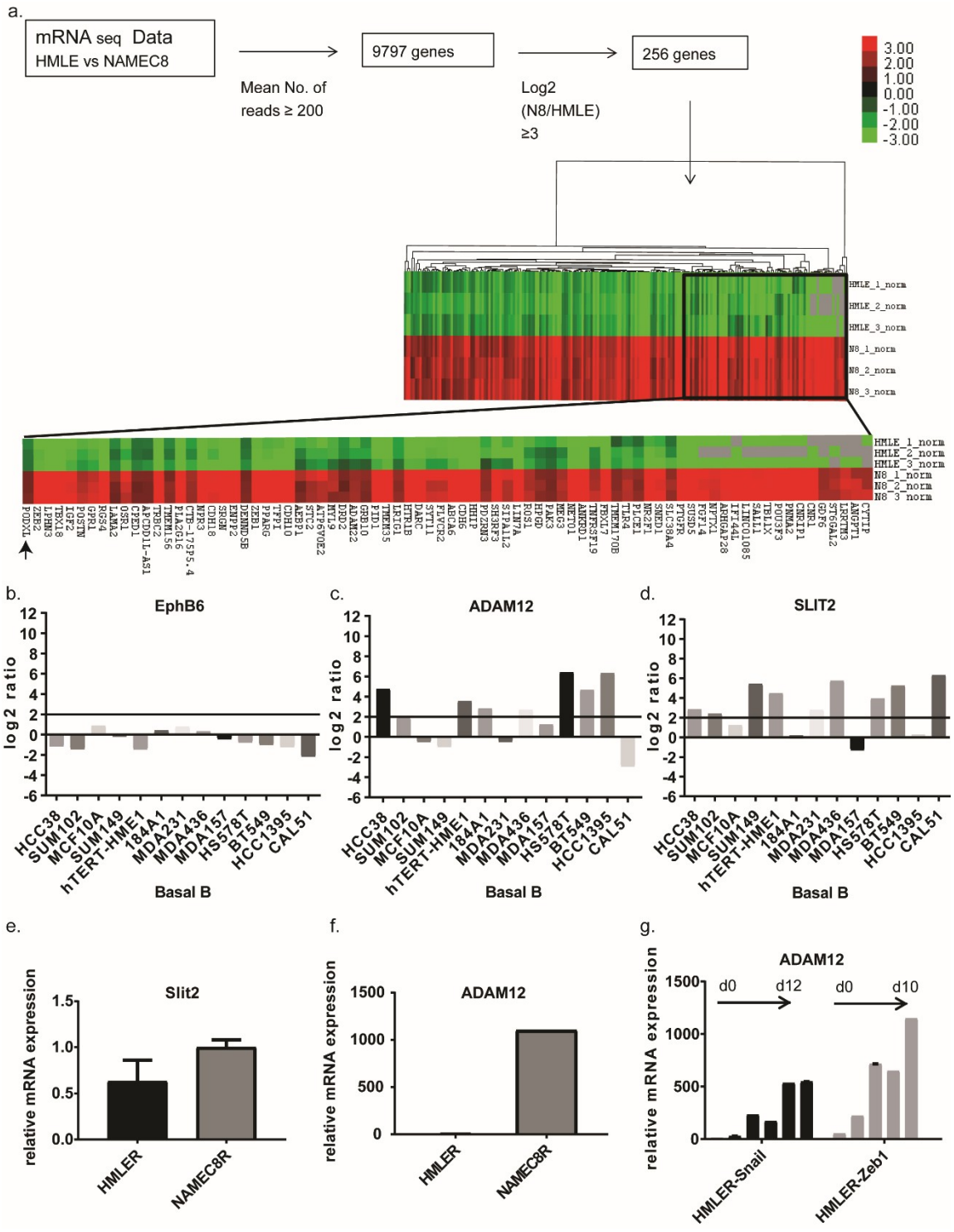

Figure S2: Candidate selection. Related to Figure 2. (a) Schematic of analysis of published gene expression data set comparing NAMEC8 and HMLE cells (Pattabiraman et al., 2016). Clustering performed with Cluster 3.0 and visualized using Java TreeView. Arrow shows *PODXL*. (b-d) mRNA expression of *EPHB6* (b) and *ADAM12* (c) and *SLIT2* (d) in breast cancer cell lines of the basal B subtype (Kao et al., 2009). (e, f) mRNA expression of *SLIT2* (e) and *ADAM12* (f) in NAMEC8R compared to HMLER cells. (g) Expression of *ADAM12* mRNA in HMLER cells induced to undergo an EMT through Dox-inducible expression of Snail or Zeb1 EMT-TFs over a time course of 10-12 days (monitored at 2-day intervals). Normalized to Day 0.

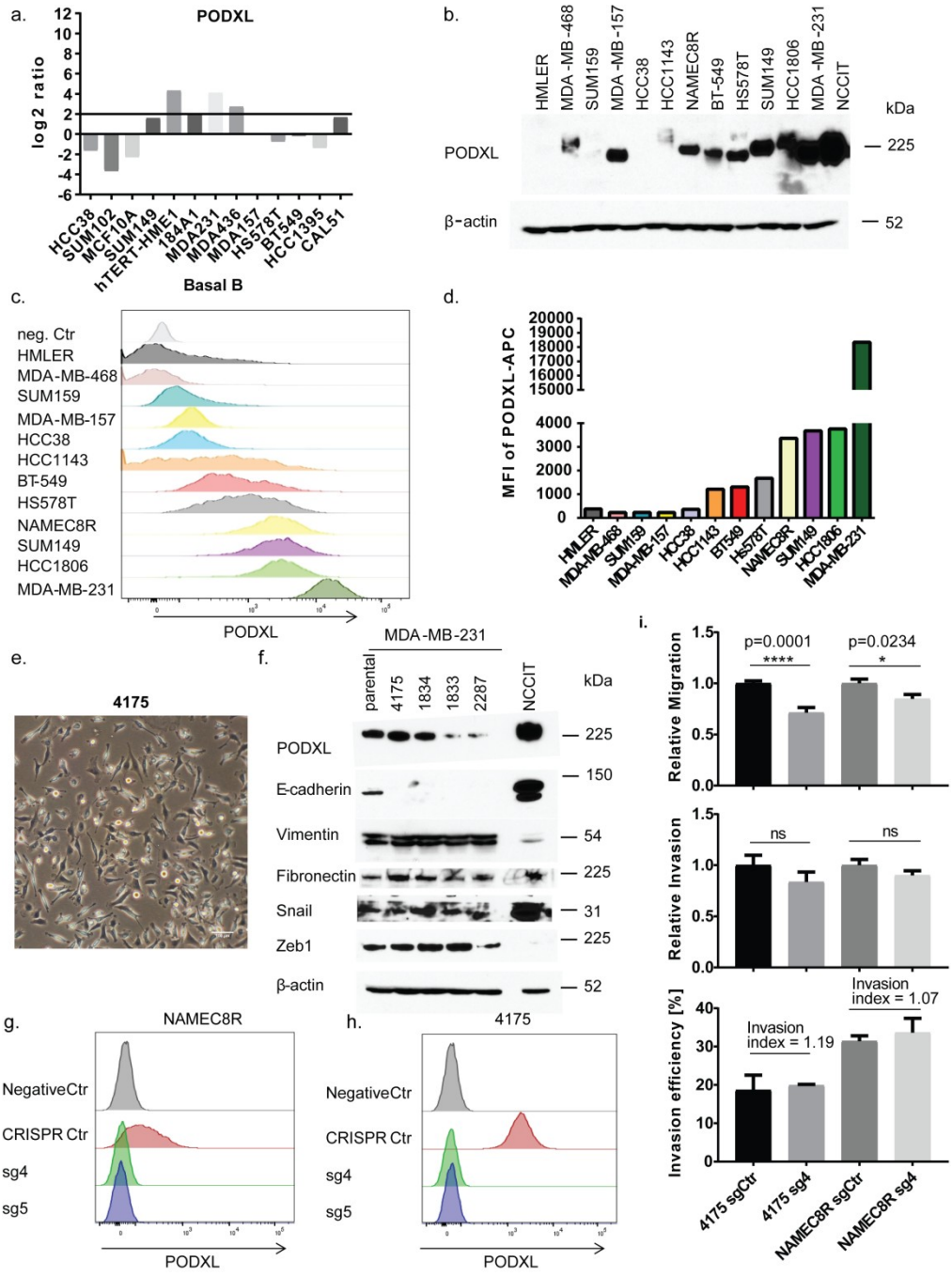

Figure S3: PODXL mRNA and protein expression in basal breast cancer cell lines. Related to Figure 2 and 3. (a) mRNA expression of *PODXL* in breast cancer cell lines of the basal B subtype (Kao et al., 2009). (b-d) PODXL protein levels in a panel of breast cancer cell lines as determined by Western blot analysis (b) and flow cytometry (c, d). The MFI (mean fluorescence intensity) of PODXL was quantified for each cell line (d). (e) Bright-field image showing the mesenchymal morphology of the 4175 clone of the MDA-MB-231 cell line. Scale bar: 100 µm. (f) Protein expression of PODXL and EMT markers in different clones of the MDA-MB-231 cell line. (g, h) Flow cytometric analysis of CRISPR/Cas9-mediated KO of *PODXL* using two different guide RNAs in NAMEC8R (g) and MDA-MB-231 4175 (h) cells compared to cells expressing a control guide RNA. (i) Migration (top) and invasion (middle) analysis of NAMEC8R and 4175 cell with or without PODXL KO over a time period of 24 h. The bottom panel shows the invasion efficiency (invasion relative to migration). Representative data of three biological replicates. Data are represented as mean ± SEM (n=6) and all statistics were calculated using student's t-test.

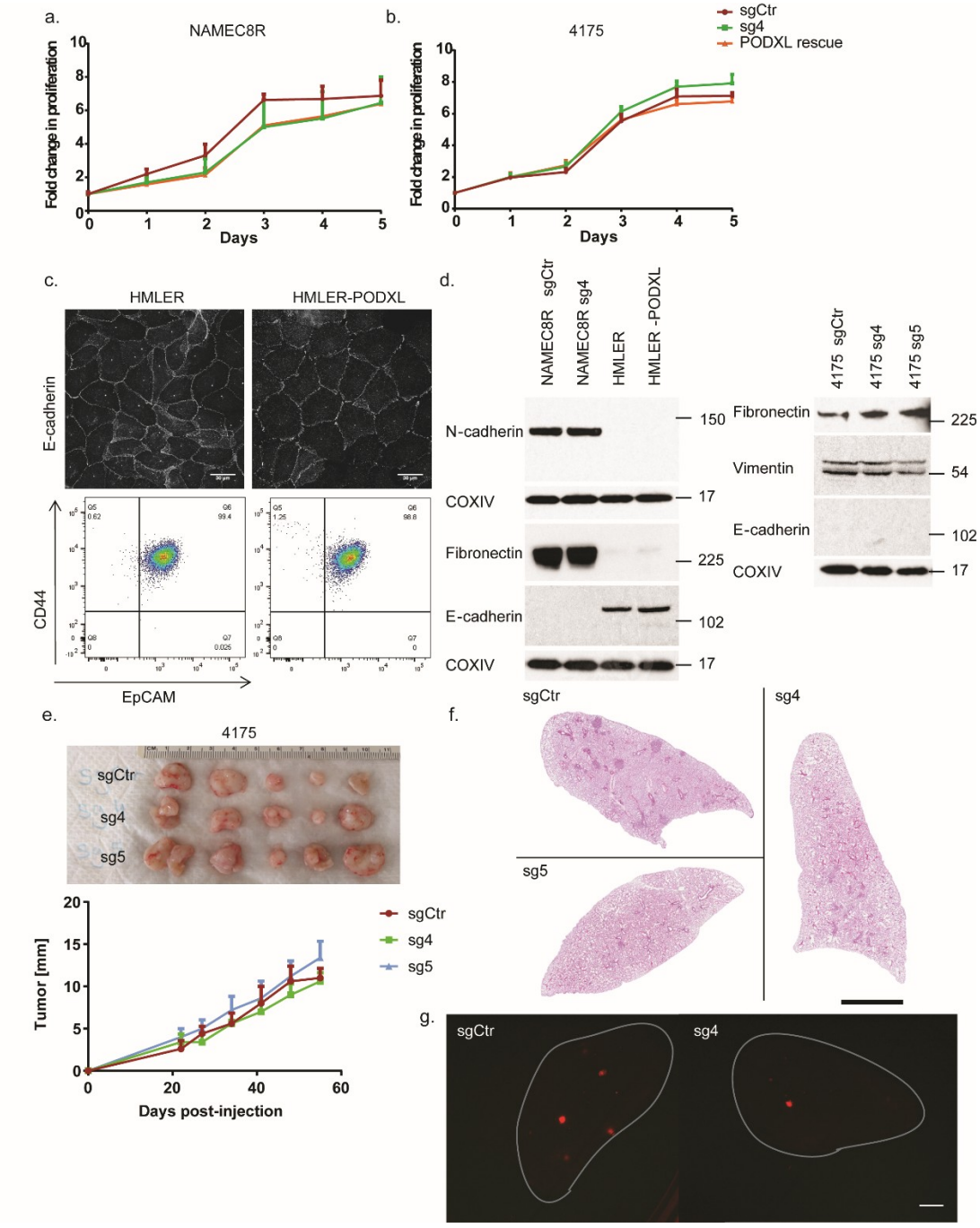

Figure S4: PODXL KO and overexpression in breast cancer cell lines. Related to Figure 3 and 5. (a, b) Proliferation of NAMEC8R (a) and 4175 (b) control cells compared to *PODXL* KO cells and KO cells re-expressing wt PODXL (PODXL rescue) over 5 days *in vitro*. (c) Top: HMLER and HMLER-PODXL cells stained for E-cadherin (grey). Scale bars: 30 µm. Bottom: Flow cytometric analysis of EpCAM and CD44 levels in HMLER and HMLER-PODXL cells. (d) Western blot analysis of EMT markers in breast cancer cells with either KO of *PODXL* or *PODXL* overexpression. (e) Primary tumors formed after orthotopic injection of $1x10^5$ 4175 cells with or without PODXL KO into the mammary fat pad of NOD/Scid mice (n=5). Tracking of tumor growth over time revealed no differences in growth rate. (f) Representative images of metastatic nodules in the lungs of mice formed by MDA-MB-231 4175 cells as seen in H&E-stained lung sections 5 weeks post-injection. Scale bar = 1 cm. (g) Representative images of tdTomato-positive metastatic nodules formed by tdTomato-positive NAMEC8R cells in the lungs of mice 6 weeks post-injection. Scale bar = 1 cm.

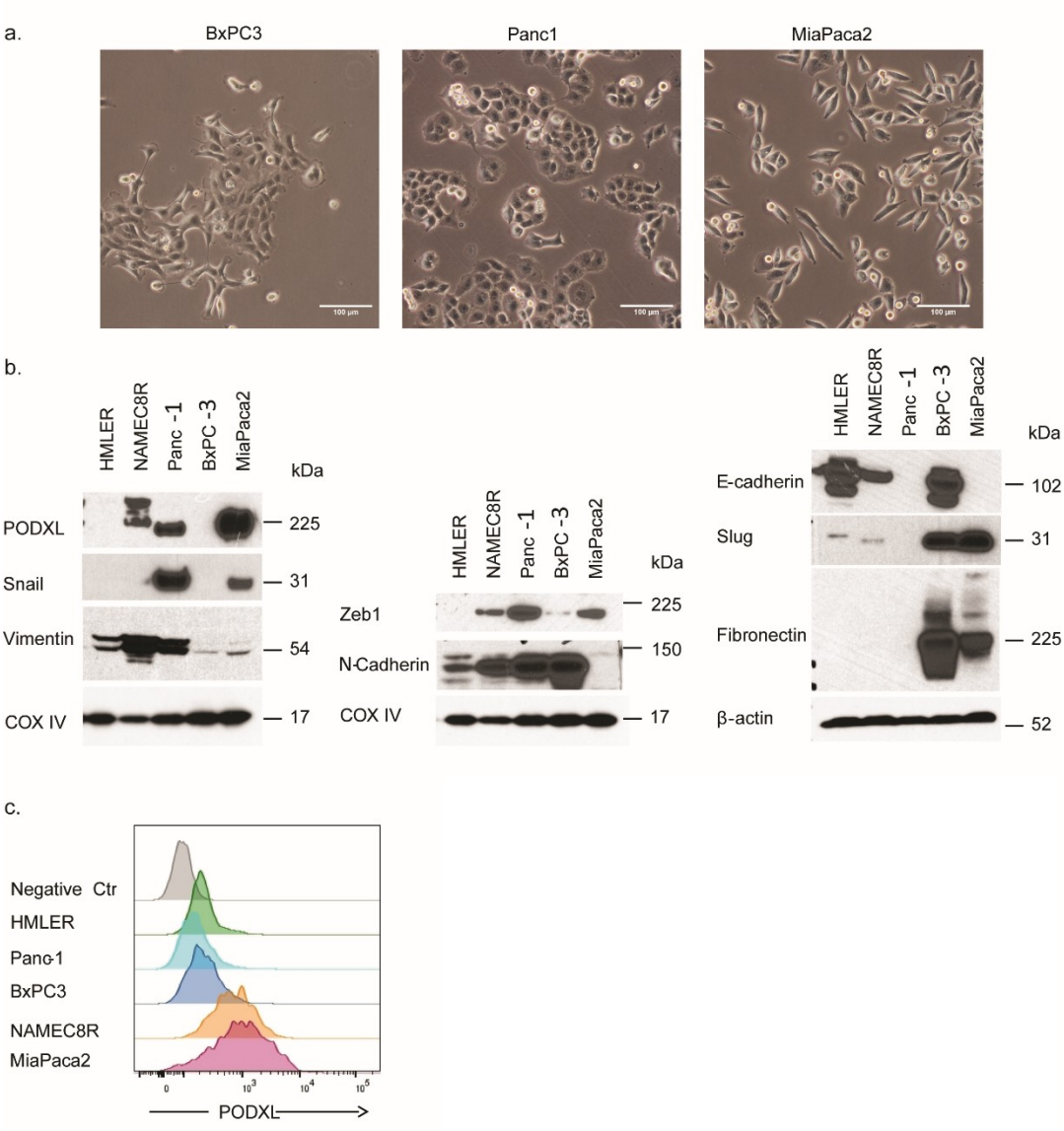

Figure S5: EMT and PODXL in pancreatic cancer cell lines. Related to Figure 4. (a) Bright-field images showing the morphology of three pancreatic cancer cell lines growing in monolayer: BxPC3, Panc1 and MiaPaca2. Scalebars: 100 µm. (b) Western blot comparing protein expression of PODXL and EMT markers in HMLER and NAMEC8R breast cancer cell lines with three pancreatic cancer cell lines. The two mesenchymal pancreatic cancer cell lines, Panc-1 and MiaPaca2, express high levels of PODXL. (c) Flow cytometric analysis of PODXL cell surface levels in breast and pancreatic cancer cell lines.

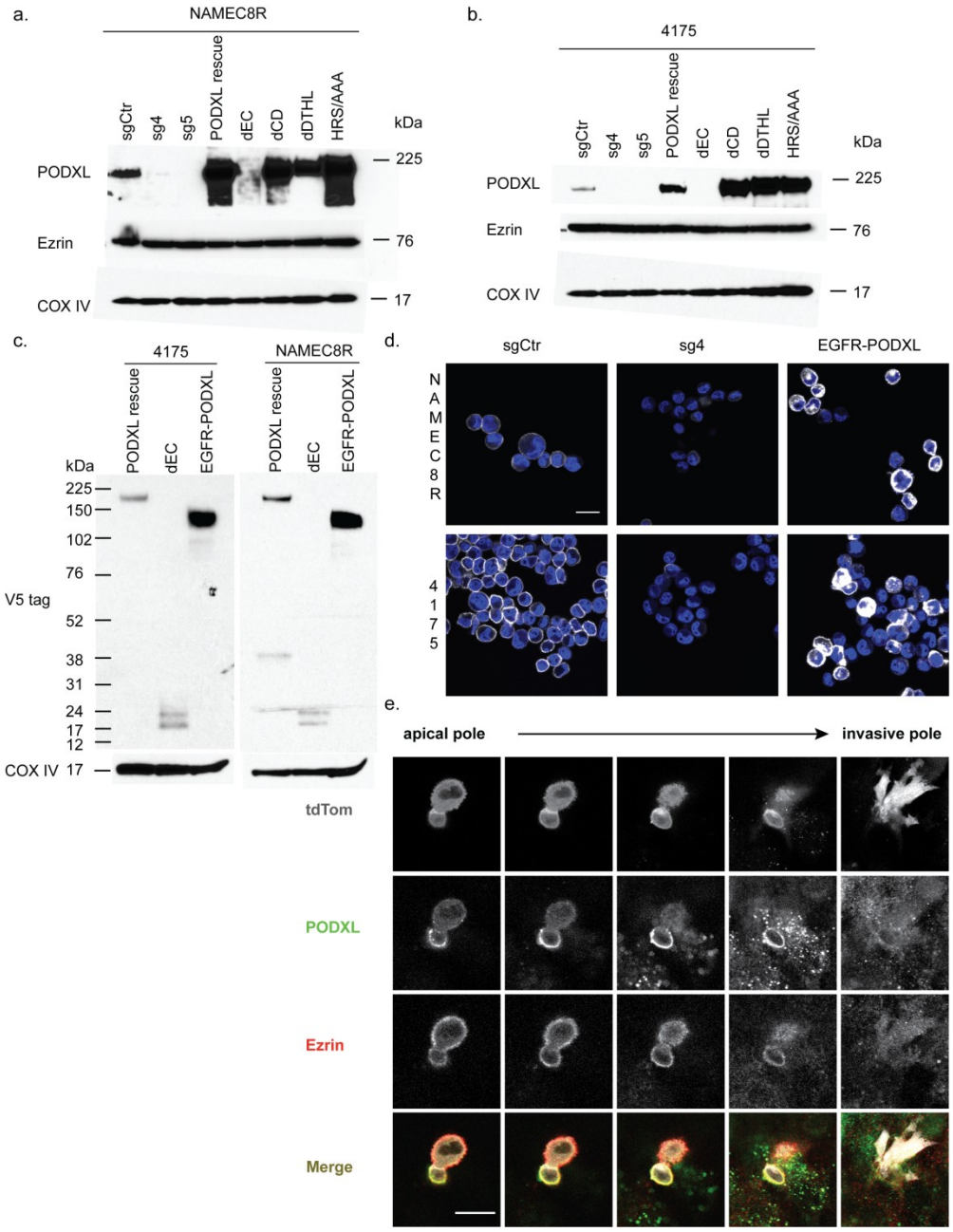

Figure S6: Expression of PODXL mutants in PODXL KO carcinoma cells. Related to Figure 6.
(a, b) Western blot analysis of PODXL and ezrin protein levels in NAMEC8R (a) and 4175 (b) cells with (sg4, sg5) or without (sgCtr) PODXL KO and KO cells expressing either wt PODXL (PODXL rescue) or different PODXL mutants. The antibody against PODXL recognizes the extracellular domain of the protein. (c) Western blot analysis of PODXL protein levels in NAMEC8R and 4175 expressing V5-tagged wt (PODXL rescue), a V5-tagged mutant PODXL with extracellular domain deletion (dEC) or a V5-tagged EGFR-PODXL fusion protein. (d) Immunofluorescent staining of cell surface PODXL (sgCtr and sg4) or V5-tagged EGFR-PODXL fusion protein in NAMEC8R cells and MDA-MB-231 4175 cells. The EGFR-PODXL fusion protein is expressed on the cell surface of the breast cancer cells. Scalebar: 20 µm. (e) NAMEC8R sgCtr cell transmigrating through HUVEC monolayer into 3D collagen gel. The cell expressed tdTomato (grey) and was stained for ezrin (red) and PODXL (green). A gallery of single xy sections taken at 2.1 µm intervals from the apical to the invasive pole is shown. Scale bar: 20 µm. Note that the HUVECs also stain positive for PODXL and ezrin.

Supplemental Methods

CRISPR/Cas9-mediated knockout

NAMEC8R and 4175 with PODXL knockout (KO) cell lines were generated by lentiviral transduction with the lentiCRISPRv2 backbone (Sanjana et al., 2014) (lentiCRISPR v2 was a gift from Feng Zhang (Addgene plasmid # 52961)) containing target sequences against Exon 1 (sg5) or Exon 2 (sg4) Following lentiviral infection, successful KO of PODXL was confirmed by flow cytometric analysis and western blot analysis of PODXL. Homogeneous cancer cell populations with PODXL KO were acquired by FACS.

Small guide RNAs for CRISPR/Cas9-mediated knock-out

Gene	Sequence Source	Score	Forward	Reverse	Target	Number
Non-coding	GeCKO-V2 Library HGLibA_6403	-	CACCGGTGTCGGATTCCGCCGCTTA	AAACTAAGCGGCGGAATCCGACACC	-	1070
Non-coding	GeCKO-V2 Library HGLibA_64407	-	CACCGCTATCTCGAGTGGTAATGCG	AAACCGCATTACCACTCGAGATAGC	-	1071
PODXL	sgRNA Designer (Broad)	0.77	caccgGTGTATCCAGTGACTCACCG	aaacCGGTGAGTCACTGGATACACc	Exon2	Sg4
PODXL	sgRNA Designer (Broad)	0.61	caccgTCACCATTCTGGGAGGGCGA	aaacTCGCCCTCCCAGAATGGTGAc	Exon1	Sg5

Q5 site-directed mutagenesis

Rescue of PODXL KO cells with active Cas9 was achieved by re-expression of PODXL containing a silent mutation in the PAM recognition site previously used by Cas9. For this purpose, the Gateway entry vector pENTR233_PODXL was used to produce pENTR233_PODXL G273C using the Q5 site-directed mutagenesis kit (NEB #E0554S). pENTR233_PODXL was provided by the ORFeome Collaboration (PlasmID clone ID HsCD00378744, PMID 17207965 and 154893350; Storage and distribution provided by the PlasmID Repository at Harvard Medical School and funded in part by NCI Cancer Center Support Grant #NIH 5 P30 CA06516). Primers were designed using the NEBaseChanger Tool (NEB; see Table). Successful point mutation was confirmed by Sanger DNA sequencing. pENTR233_PODXL G273C was then recombined into the Gateway destination vector pLEX_307 (pLEX_307 was a gift from David Root; Addgene plasmid #41392) containing a V5 tag using Gateway LR clonase Enzyme mix (ThermoFischer Scientific #11791019). Other PODXL mutants were produced from pENTR233_PODXL G273C using the Q5 site-directed mutagenesis kit. The PODXL mutant dEC-PODXL that carries a deletion of the extracellular domain was additionally tagged with V5. The DNA sequences of the PODXL mutants were confirmed by sequencing and the gateway entry vectors were recombined into the Gateway destination vector EBFP membrane.
Lentivirus was produced of all constructs using standard methods (Stewart et al., 2003) and NAMEC8R sg4 and 4175 sg4 cells were stably transduced with the PODXL mutants and sorted for similar cell surface expression/BFP expression by FACS.

Primers for Q5 site-directed mutagenesis

Mutant	Forward	Reverse
PODXL PAM mutant	ACTCACCGGGCACTACAACCC	CACTGGATACACCAAGGG
dEC-PODXL	CCCCTCATCATCACCATC	CAACTTTTTTGTACAAAGTTGG
dEC-PODXL-V5	GCTGGGCCTGGATAGCACCTAGCC AACTTTCTTGTACAAAG	AGCGGGTTCGGAATCGGTTTGCCCA AGAGGTGTGTGTCTTC
PODXL-dCD	CCAACTTTCTTGTACAAAGTTGG	GCAGCAGCCATAGAGGGC
PODXL-dDTHL	CCAACTTTCTTGTACAAAGTTGG	CTCCTCATCCAGGTCGTC
PODXL-HRS/AAA	GGCACTCGCACAGAGGAAGGACCA GCAGC	TGTGCGCAGCAGCCATAGAGGGCCG CCAC

RNA interference using shRNAs

NAMEC8Rs with PODXL or ezrin KD were generated via lentiviral infection with pLKO.1 puro containing shRNA sequences (Addgene plasmid #8453; see Table for shRNA sequences). Control cell lines were generated via lentiviral infection with pLKO.1 TRC control, a gift from David Root (Addgene plasmid #10879; (Moffat et al., 2006)). NAMEC8Rs with ADAM12 KD and control cells were generated with lentiviral infection using GIPZ plasmid purchased from Dharmacon. Briefly, NAMEC8Rs were transduced using lentivirus generated by transfection of HEK293T cells with the viral envelope and packaging plasmids, pCMV-VSV-G (Addgene plasmid #8454) and pCMV-dR8.2 dvpr (Addgene plasmid #8455) were originally developed in the Weinberg lab (Stewart et al., 2003). KD efficiency was assessed using qRT-PCR.

shRNA sequences

Primer	Target	Sequence
shTRC Ctr Fwd	Non-targeting	CCGGCCGCAGGTATGCACGCGTCTCGAGACGCGTGCATACCTGCGGTTTTTG
shTRC Ctr Rev	Non-targeting	AATTCAAAAACCGCAGGTATGCACGCGTCTCGAGACGCGTGCATACCTGCGG
sh9 Fwd	PODXL	CCGGAGCCACGTAAGGGACTTTATACTCGAGTATAAAGTCCCTTACGTGGCTTTTTTG
sh9 Rev	PODXL	AATTCAAAAAAGCCACGTAAGGGACTTTATACTCGAGTATAAAGTCCCTTACGTGGCT
sh11 Fwd	PODXL	CCGGACGAGCGGCTGAAGGACAAATCTCGAGATTTGTCCTTCAGCCGCTCGTTTTTTG
sh11 Rev	PODXL	AATTCAAAAAACGAGCGGCTGAAGGACAAATCTCGAGATTTGTCCTTCAGCCGCTCGT
sh22 Fwd	Ezrin	CCGGCCCACGTCTGAGAATCAACAACTCGAGTTGTTGATTCTCAGACGTGGGTTTTTG
sh22 Rev	Ezrin	AATTCAAAAACCCACGTCTGAGAATCAACAACTCGAGTTGTTGATTCTCAGACGTGGG
sh23 Fwd	Ezrin	CCGGCGTGGGATGCTCAAAGATAATCTCGAGATTATCTTTGAGCATCCCACGTTTTTG
sh23 Rev	Ezrin	AATTCAAAAACGTGGGATGCTCAAAGATAATCTCGAGATTATCTTTGAGCATCCCACG
GIPZ Ctr Fwd	Non-targeting	ATCTCGCTTGGGCGAGAGTAAG
GIPZ Ctr Rev	Non-targeting	CTTACTCTCGCCCAAGCGAGAG
Sh-13 GIPZ (Dharmacon)	ADAM12	TTGACATTGACGATTCAGG
Sh-14 GIPZ (Dharmacon)	ADAM12	TTTATGATCAGTTCTTTGC

Plasmid Constructs and Virus Production

Plasmid	Producer
pCMV-dR8.2 dvpr (Packaging plasmid for Lentiviral constructs)	Addgene plasmid #8455 (Stewart et al., 2003)
pCMV-VSV-g (Envelope plasmid for Lentiviral constructs)	Addgene plasmid # 8454 (Stewart et al., 2003)
pUMVC (Packaging plasmid for Retroviral constructs)	Addgene plasmid # 8449 (Moffat et al., 2006)
pFUW-LPT2 Zeb1	Z. Keckesova
pFUW-LPT2 hSnail	Z. Keckesova (Lu et al., 2014 Nov)
pLEX_307	Addgene plasmid #41392
pcDNA3.1(+)/Luc2=tdT	Addgene plasmid #32904
pENTR1A Dual Selection Vector	ThermoFischer Scientific #A10462
lentiCRISPRv2	Addgene plasmid #52961 (Sanjana et al., 2014)
pENTR223_PODXL	PlasmID Repository at Harvard Medical School (HsCD00378744)
pGIPZ	Dharmacon
pLKO.1 puro	Addgene plasmid #8453 (Stewart et al., 2003)
pLKO.1 TRC control	Addgene plasmid #10879 (Moffat et al., 2006)
pLV-clover-mouse Par1b	T. Shibue
pLV-clover mouse PKC-iota	T. Shibue
Gateway Dest. EBFP mem	B. Bierie
pLV-lifeact-mRuby2	T. Shibue (Shibue et al., 2012)
pWZL-HRAS(G12V)-Blast	W.L. Tam (Tam et al., 2013)

Western Blot Analyses

Cell were harvested in RIPA buffer containing phosphatase inhibitors 2/3 (1:100; Sigma-Aldrich #P5726 & #P0044) and protease inhibitor (1:100; Sigma Aldrich #P8340). NUPAGE Bis-Tris Mini Gels (ThermoFischer Scientific) were transferred to PVDF membranes using XCell II mini cell apparatus and blocked in 5% non-fat dry milk/TBS-T. Membranes were incubated with antibodies overnight, as recommended for each antibody protocol. Membranes were washed with TBS-T, and incubated with secondary antibody in 5% non-fat dry milk/TBS-T for 1 hour at room temperature, followed by washing and detection via ECL reagent.

Antibodies for Western Blot Analyses

Antibody	Specifity	Dilution	Method	Producer
Mouse anti human PODXL	Total PODXL (extracellular epitope)	1:500 (5% Milk/ TBS-T)	Western blot	Santa Cruz #sc-23904
Mouse anti-human Ezrin	Total Ezrin	1:1,000 (5% Milk/ TBS-T)	Western blot	Sigma Aldrich #E-8897
Rabbit anti-human COX IV	Total COX IV	1:5,000 (3% BSA/TBS-T)	Western blot	Cell Signaling Technology #4850
rabbit anti-human GAPDH	total GAPDH	1:5,000 (5% BSA/TBS-T)	Western blot	Cell Signaling Technology #2118S
Rabbit anti-human E-cadherin	E-cadherin	1:1,000 (5% BSA/TBS-T)	Western blot	Cell Signaling Technology #3195
Mouse anti-human N-cadherin	N-cadherin	1:1,000 (5% BSA/TBS-T)	Western blot	BD Pharmingen #610921
Mouse anti human-Fibronectin	Fibronectin	1:1,000 (5% BSA/TBS-T)	Western blot	BD Biosciences #610078
Rabbit anti-human Vimentin	Vimentin	1:1,000 (5% BSA/TBS-T)	Western blot	Cell Signaling Technology #3932
Rabbit anti-human Zeb1	Zeb1	1:1,000 (5% BSA/TBS-T)	Western blot	Cell Signaling Technology #3396
Rabbit anti-human Snail	Snail	1:1,000 (5% BSA/TBS-T)	Western blot	Cell Signaling Technology #3879
Mouse anti-V5 tag [GT1071] antibody	V5 tag	1:1,000 (5% Milk/TBS-T)	Western blot	GeneTex #GTX628529
Rabbit anti-human MARK2 (Par1b)	MARK2/Par1b	1:1,000 (5% BSA/TBS-T)	Western blot	Cell Signaling Technology #9118S
Biotinylated anti-mouse IgG, HRP-coupled	Mouse IgG	1:10,000 (5 % Milk in 1 M TBS-T)	Western blot	Cell Signaling Technology #7076S
Biotinylated anti-rabbit IgG, HRP-coupled	Rabbit IgG	1:5,000 (5 % Milk in 1 M TBS-T)	Western blot	Cell Signaling Technology #7074P2

FACS

The cells were prepared and stained according to standard protocols and suspended in 5% IFS/PBS. For staining of PODXL, cells were detached using an enzyme-free cell dissociation buffer (ThermoFischer Scientific, #13151014) instead of trypsin. Cells were sorted on BD FACSAria SORP and analyzed on BD LSRII, using BD FACSDiva Software (BD Biosciences). Data were processed and analyzed using Flowjo (Flowjo LLC). Antibodies used are ms anti-PODXL-Alexa647 (Nuromab; CureMeta), CD44-PE-Cy7 (Biolegend #103029), EpCAM-PacificBlue (Biolegend #324218), CD104-PE (Biolegend #327808) at 1:100 dilution and CD24-FITC (BD Pharmingen #555427) at 1:30 dilution for 30 minutes in 5% IFS/PBS.

Migration, invasion and transendothelial migration assays

For transendothelial migration assays, FluoroBlok transwells (Corning Life Sciences, #351152) were coated with collagen, seeded with $5x10^5$ HUVECs and cultured at 37°C, 5% CO_2 for 24 h. Tightness of the endothelial monolayer was tested on two HUVEC-coated transwells by FITC-Dextran (EMD Millipore #90328) permeability following the guidelines of the FITC-Dextran vascular permeability assay (EMD Millipore #ECM644) and compared to an empty transwell. The other transwells containing HUVEC monolayers were seeded with $5x10^4$ fluorescently labeled cancer cells, incubated for 24 h and the successfully transmigrated cells were counted using the Axio Observer A1 microscope (Zeiss). Per transwell, 3 fields of view at 10x magnification were analyzed.

For migration assays, $5x10^4$ cancer cells were seeded into transwells (Corning Life Sciences, #353097). For invasion assays, transwells containing dehydrated matrigel (Corning Life Sciences, #354483) were rehydrated according to protocol prior to cancer cell seeding and then seeded like migration assays. The seeded transwells were incubated for 24 h, fixed in methanol and transmigrated cancer cells were stained using crystal violet (0.01%) in 20% methanol. Per transwell, 3 fields of view at 10x magnification were counted using the Axio Observer A1 microscope (Zeiss). In order to correct for differences in cell numbers due to seeding errors and proliferation, cancer cells of the same cells solution used to seed the migration/invasion/transendothelial migration assay were seeded for a proliferation assay for 24 h and the average number of cells per cell type was determined using CyQuant (Thermo Fisher Scientific, C7026). The normalized cell counts were then used to correct the number of transmigrated cells and data were plotted using GraphPad Prism.

Proliferation assay

Proliferation assays were conducted in 96-well plates using CyQuant (Thermo Fisher Scientific, C7026), according to the manufacturer's recommendations, to measure DNA content in each well during a 5-d time course. The first day after seeding was counted as *Day 0* and used for normalization of values obtained from plates collected at subsequent time points.

Immunofluorescent staining of cancer cell migration through HUVEC monolayers cultured on collagen I gels

For immunofluorescent staining of proteins, samples were fixed after 3 h of co-culture using 4 % PFA for 20 min at room temperature (RT) and stained as previously described (Artym and Matsumoto, 2010). Primary antibodies used were mouse anti-PODXL (Santa Cruz, #sc-23904), mouse anti-Ezrin (Santa Cruz, #sc-58758) at 1:50 and rabbit anti-Ezrin (Cell Signaling Technology #3145) at 1:50. Cells were imaged using the LSM710 confocal microscope (Zeiss). Multiple z-stacks were acquired per well at different locations using a 63x oil objective and analyzed using Imaris software (Bitplane).

Immunohistochemistry

Tissue microarrays BR1503e and BRM961a were purchased from US Biomax, Inc.. Slides were rehydrated in a descending alcohol series. Antigen retrieval of tissue sections was performed at 125°C for 20 min in pH 6.0-Sodium citrate buffer, washed with PBS and endogenous peroxidase activity was blocked using BLOXALL endogenous peroxidase and alkaline phosphatase blocking solution (Vector Laboratories, #SP6000). After washing, endogenous streptavidin/biotin was blocked using a streptavidin/biotin blocking kit (Vector Laboratories SP-2002). Following another washing step, the microarrays were blocked using Background Terminator (Biocare Medical #BT967 H,L) for 7 min at RT to reduce nonspecific antibody binding. Slides were then washed three times. All wash steps were performed with PBS. Staining was performed at 4°C over night using biotin-labeled monoclonal mouse anti-human PODXL antibody (1:50 in PBS; CureMeta). Following three wash steps, slides were incubated with ABC reagent (Vector Laboratories, Vectastain Elite ABC-HRP kit (Peroxidase, mouse IgG) #PK-6102) for 30 minutes at room temperature. Peroxidase reaction was performed using ImmPACT DAB peroxidase substrate (Vector Laboratories #SK-4105) and the reaction was stopped with diH_2O. Tissues were then counterstained using hematoxylin QS (Vector Laboratories #H-3404). Following dehydration in an ascending alcohol series, slides were mounted in Vectamount Mounting Medium (Vector Laboratories #H-5000). For imaging, slides were scanned using the Aperio Digital Pathology slide scanner (Leica Biosystems) and analyzed using the Aperio Image Scope (Leica Biosystems) software.

Immunofluorescence (IF) on suspended cells

Cancer cells were harvested using an enzyme-free cell dissociation buffer (ThermoFischer Scientific, #13151014) and pelleted at 3000 rpm for 5 min by centrifugation. The cells were then fixed by addition of 4% PFA for 10 min at RT under rotation. Following two washing steps with PBS, cells were blocked in 50 µl blocking buffer (10 % HS + 3 % BSA) for 30 min at RT under rotation. Next, the primary antibodies ms anti-PODXL-Alexa647 (Nuromab, CureMeta) or ms anti-V5 tag [GT1071] (GeneTex #GTX628529) were diluted at 1:50 in blocking buffer and 50 µl were added to each sample. Samples were incubated over night at 4°C under rotation. On the next day, cells were washed four times with PBS and then stained with DAPI (1:1000 in blocking buffer) for 10 min at RT or with DAPI (1:1000 in blocking buffer) and gt anti-ms A647 (Invitrogen #A21235; 1:200 in blocking buffer). Cells were washed three times with PBS and then resuspended in 10 µl ProLong Gold antifade mounting medium with DAPI (Lifetech

#P36931) and loaded onto histology slides and coverslipped. Samples were air dried and stored at 4°C prior to imaging with LSM700 confocal microscope (Zeiss).

Quantitative Real time PCR (qRT-PCR)

RNA extraction was performed on collected cell pellets according to the guidelines of the Qiagen RNeasy® Plus extraction protocol. The purified RNA was reverse transcribed into cDNA using a high-capacity cDNA reverse transcription kit (Applied Biosystems #4368814) according to the manufacturers guidelines. In total, 1 µg RNA per sample was reverse transcribed using the MyCycler Thermal Cycler. In order to analyze the expression levels of several proteins, the cDNA was diluted by the addition of 80 µl H_2O to a final volume of 100 µl. For each reaction 2 µl of each cDNA sample were mixed with 10 µl LightCycler 480 SYBR Green I Master mix (2 x), 6.4 µl H_2O and 1.6 µl of forward and reverse primer mix (10 µM forward + 10 µM reverse primer). All samples were loaded on a 384 well plate and analyzed by quantitative real time PCR using the Roche Light cycler 480 II. The mRNA levels of genes of interest (e.g. PODXL) were normalized to the mRNA levels of the housekeeping gene GAPDH. The data were then analyzed using Excel and plotted with GraphPad Prism.

Primers for qRT-PCR

Gene	Forward	Reverse
GAPDH	GGTCTCCTCTGACTTCAACA	GTGAGGGTCTCTCTCTTCCT
SNAI2	TGACCTGTCTGCAAATGCTC	TCGGACCCACACATTACCTT
SNAI1	CTGGGTGCCCTCAAGATGCA	CCGGACATGGCCTTGTAGCA
TWIST1	GGAGTCCGCAGTCTTACGAG	TCTGGAGGACCTGGTAGAGG
ZEB1	CCAGGTGTAAGCGCAGAAA	CCACAATATGCAGTTTGTCTTCA
CDH1	GTCGAGGGAAAAATAGGCTG	TTGACGCCGAGAGCTACAC
FN1	AAACCAATTCTTGGAGCAGG	CCATAAAGGGCAACCAAGAG
SLIT2	AGCCGAGGTTCAAAAACGAGA	GGCAGTGCAAAACACTACAAGA
PODXL	AGCTAAACCTAACACCACAAGC	TGAGGGGTCGTCAGATGTTCT
ADAM12	CGAGGGGTGAGCTTATGGAAC	GCTTTCCCGTTGTAGTCGAATA
EZR	CTCTGCATCCATGGTGGTAA	GATAGTCGTGTTTTCGGGGA

Bioinformatic analysis of mRNA sequencing data

In order to look for cell surface proteins that are differentially expressed in cells prior to and after an EMT, a previously published mRNA sequencing data set was analyzed (Pattabiraman et al., 2016). The data set was filtered for genes that had a mean number of reads equal to or greater than 200 (=9797 genes). Furthermore, only genes that were upregulated at least 3-fold on a log2 scale were included (256 genes). Gene expression data were clustered using Cluster 3.0 and visualized using Java TreeView (de Hoon et al., 2004; Saldanha, 2004). We selected several candidate genes that might be involved in the regulation of adhesion to endothelial cells, transendothelial migration and invasion of these cells, focusing in particular on cell-surface proteins.

References

Artym, V.V., and Matsumoto, K. (2010). Imaging cells in three-dimensional collagen matrix. Current protocols in cell biology *Chapter 10*, Unit 10 18 11-20.

de Hoon, M.J., Imoto, S., Nolan, J., and Miyano, S. (2004). Open source clustering software. Bioinformatics *20*, 1453-1454.

Lu, H., Clauser, K.R., Tam, W.L., Fröse, J., Ye, X., Eaton, E.N., Reinhardt, F., Donnenberg, V.S., Bhargava, R., Carr, S.A.*, et al.* (2014 Nov). A breast cancer stem cell niche supported by juxtacrine signalling from monocytes and macrophages. Nat Cell Biol.

Moffat, J., Grueneberg, D.A., Yang, X., Kim, S.Y., Kloepfer, A.M., Hinkle, G., Piqani, B., Eisenhaure, T.M., Luo, B., Grenier, J.K.*, et al.* (2006). A lentiviral RNAi library for human and mouse genes applied to an arrayed viral high-content screen. Cell *124*, 1283-1298.

Pattabiraman, D.R., Bierie, B., Kober, K.I., Thiru, P., Krall, J.A., Zill, C., Reinhardt, F., Tam, W.L., and Weinberg, R.A. (2016). Activation of PKA leads to mesenchymal-to-epithelial transition and loss of tumor-initiating ability. Science *351*, aad3680.

Saldanha, A.J. (2004). Java Treeview--extensible visualization of microarray data. Bioinformatics *20*, 3246-3248.

Sanjana, N.E., Shalem, O., and Zhang, F. (2014). Improved vectors and genome-wide libraries for CRISPR screening. Nat Methods *11*, 783-784.

Shibue, T., Brooks, M.W., Inan, M.F., Reinhardt, F., and Weinberg, R.A. (2012). The outgrowth of micrometastases is enabled by the formation of filopodium-like protrusions. Cancer Discov *2*, 706-721.

Stewart, S.A., Dykxhoorn, D.M., Palliser, D., Mizuno, H., Yu, E.Y., An, D.S., Sabatini, D.M., Chen, I.S., Hahn, W.C., Sharp, P.A.*, et al.* (2003). Lentivirus-delivered stable gene silencing by RNAi in primary cells. RNA (New York, NY) *9*, 493-501.

Tam, W.L., Lu, H., Buikhuisen, J., Soh, B.S., Lim, E., Reinhardt, F., Wu, Z.J., Krall, J.A., Bierie, B., Guo, W.*, et al.* (2013). Protein kinase C alpha is a central signaling node and therapeutic target for breast cancer stem cells. Cancer Cell *24*, 347-364.